Effects of Organo-Clay Modifier on Physical–Mechanical Properties of Butyl-Based Rubber Nano-Composites

Ali Samadi, Mehdi Razzaghi Kashani

Department of Chemical Engineering, Polymer Engineering Group, Tarbiat Modares University, Tehran, Iran

Received 5 April 2009; accepted 2 November 2009
DOI 10.1002/app.31768
Published online 7 January 2010 in Wiley InterScience (www.interscience.wiley.com).

ABSTRACT: Bladders are important rubber parts used for shaping and curing of tires. These parts are exposed to high temperature, high pressure, medium-large extension, and oxidative aging during their service life. Curing bladders are usually made of butyl-based rubber compounds vulcanized with phenolic resin vulcanization systems. To study the effect of Montmorillonite nano-clay on properties of these rubber parts and their functionality during service, the most compatible and well dispersed organically modified Montmorillonite (OMMT) nano-clay has to be selected. To study the effects of organic modifier on properties of these compounds, five types of commercial OMMT were mixed with the compounds using the melt intercalation method. Effect of modifiers on compatibility between clay and rubber, dispersion of clay in the polymer matrix, and thus mechanical properties of the nano-composite were studied by X-ray diffraction (XRD), scanning electron microscopy (SEM), atomic force microscopy (AFM), mechanical tension, and dynamic-mechnical-thermal analysis (DMTA). XRD results revealed an intercalated structure for all OMMTs, but with different degrees of rubber intercalation. The largest change in interlayer spacing of silicate layers due to intercalation of rubber was seen for an OMMT modified by dimethyl-benzyl-hydrogenated tallow, quaternary ammonium. AFM and SEM micrographs of the latter compound confirmed the intercalated structure with a good distribution of filler. Viscoelastic properties obtained from DMTA confirmed more compatibility between butyl-based rubber compound and this OMMT. This modified clay was selected as the filler of choice for potential application in actual bladder compound. Uni-axial tension tests could also differentiate among nano-composites reinforced with differently modified clays. J Appl Polym Sci 116: 2101–2109, 2010

Key words: tire curing bladders; butyl rubber; montmorillonite organo-clay; polymer nano-composites; physical–mechanical properties

INTRODUCTION

In recent years, organically modified layered silicates (organo-clays) are increasingly used for reinforcement of polymeric materials. The dispersion of such layered silicates at the level of a few nanometers induces a significant improvement in mechanical properties, flame resistance and barrier properties, compared with virgin polymer or conventional micro and macro-composites.[1–4] Other improved properties make some potential applications of polymer-clay nano-composites in anticorrosion coating,[5,6] electrorheologically sensitive fluids,[7,8] and biodegradable materials.[2] In addition, these improvements may be obtained with low clay loading (typically 3–5%) which makes the final part lighter in weight. Furthermore, at an optimum filler loading, proper filler-polymer interaction induces reinforcing effects with minimum harmful effect of filler–filler interaction and aggregation.[9] There are several techniques used for dispersing organo-clays at a nano-scopic scale to prepare nano-composites, including addition of the organo-clay during polymerization (in situ polymerization),[10] in a solvent-assisted mixture (solution blending),[11] to a polymer melt (melt intercalation),[12] or to a co-coagulating of rubber latex (emulsion compounding).[13] Melt intercalation is the most practical method employed in the rubber industry. Nano-composite preparation via polymer melt intercalation involves heat treatment, statically or under shear, of a mixture of polymer and layered silicate above the softening point of the polymer, and it was first demonstrated by Giannelis et.al.[14] Montmorillonite (MMT) is one of the most commonly used organically modified clays in melt blending, and it is comprised of silicate layers with large surface-to-volume ratio (80–300 m^2/g) with a tactoid structure of several tens of stacked layers. These layers have a typical lateral dimension of 100–200 nm and a layer thickness around 0.96 nm.[1–3] The sum of a layer and an interlayer represents the repeat unit of the stacked material, called d-spacing or basal spacing (d001), and is calculated from the (001) harmonics obtained from X-ray diffraction (XRD) patterns.[1–3] The peaks, corresponding to crystalline structure of clay, can be easily observed by

Correspondence to: M. Razzaghi Kashani (mehdi.razzaghi@modares.ac.ir).

XRD at their diffraction angles defined by their natural spacing. Intercalation of polymer may disturb their structure from parallel and evenly spaced arrangement. If the layers exfoliate and high levels of nanoscale dispersion occur, typically both of these conditions are lost and the low-angle XRD peaks disappear. In the case where polymer chains intercalate into the layer's gallery and expand the interlayer spacing, if the layers keep their parallel and evenly spaced structure (ordered intercalated), shifted XRD peaks are detectable. However, if the layers lose their parallel configuration in intercalated systems (disordered intercalated), similar to exfoliation case, the low-angle peaks in XRD disappear without true exfoliation.[15–18] In the later case, application of other complementary techniques such as transmission electron microscopy (TEM) or Atomic Force Microscopy (AFM) become necessary to confirm the structure.[19] If dispersion of clay does not take place, the diffraction peak remains at its initial position corresponding to that of the original organo-silicate. Finally, degradation of either the polymer or the silicate modifier, for instance during vulcanization, may result in layer collapse and reduction of interlayer spacing compared to that of the original organo-silicate.[17] The intercalated/exfoliated structure of layered silicates is controlled by the compatibility between polymer and clay and processing variables.[20] When peaks are observed in XRD pattern, useful information about polymer intercalation and clay dispersion can be attained. However, complete exfoliation is an uncommon situation in melt intercalation method, nevertheless property improvement is achievable without perfect exfoliation, as long as the effective aspect ratio and surface area of the filler after mixing in rubber remain reasonably high.[17,21] The clay is naturally a hydrophilic material. Therefore, dispersion of clay in hydrophobic rubber needs surface treatment of silicate layers to give some hydrophobicity to the surface of clay and provide thermodynamic driving force for the polymer to diffuse between layers. Generally, this can be done by ion-exchange reactions with cationic surfactants, including primary, secondary, tertiary and quaternary alkylammonium cations.[22–24] These organic alkylammonium cations reduce the surface energy of clay and improve wet-ability of the clay by the typical nonpolar or mildly polar rubber. In addition, this modification results in expansion of the basal spacing due to the presence of alkyl chain intercalated in the interlayer.[22,23] In addition to commercially available organically modified MMTs, some researchers have modified this nanoclay for stronger chemical bonds between clay and rubber or more dispersion of clay layers during compounding.[25–29] Different amine type modifiers were used to modify clay for better dispersion in SBR through emulsion compounding.[25] In another work, octadecylamine was used to modify MMT and compare its efficiency in dispersion of clay in SBR with melt intercalation and emulsion compounding methods.[26] There are some practical works in which an amine having at least two amine centers as a cationic polymeric quaternary amine or ethylene polyamine or cationic polyelectrolyte were used in situ during emulsion compounding to promote exfoliated structure of nanoclay and prevent reagglomeration of clay platelets during coagulation process.[27,28] Also a low molecular weight siloxane surfactant was employed to modify clay for achieving exfoliation structure in silicone rubber.[29]

Tire curing bladder is one of the important rubbery components used in curing presses in tire processing. It is an expandable hollow-shaped component, usually made of butyl-based rubber compounds, vulcanized by phenolic resin systems (to impart good resistance to heat and ozone/oxygen attacks). This rubbery part is used as a heat transfer and shaping medium during curing of a green tire, and it is used under demanding conditions of, either high-pressure steam (1.23–1.93 MPa), hot water (190°C and 2.74 MPa), a combination of both, or heated nitrogen.[30,31] After curing a tire, bladder has to return to its original shape for another cure cycle, so dimensional stability of bladders guarantees proper shaping and curing of tires. Therefore, thermo-mechanical as well as time-dependent properties of bladders are crucial in their quality of performance, duration of service, and possible damages on tires due to their failures. In addition to the cross-linked network of rubber molecules, reinforcing filler network can define time-dependent properties of bladder compounds such as creep and permanent set.[30,32,33] Therefore, a detailed study of the properties of the bladder compound is essential. In the current study, a proper type of organically modified Montmorillonite (OMMT) nano-clay was selected by studying the effect of modifier type on dispersion of the clay in a butyl-based rubber matrix through assessment of the degree of intercalated structure of OMMT using XRD and morphology of the selected nano-composite by SEM and AFM. Commercial organoclays are used since their dispersion in butyl rubber is limited to melt blending in the tire industry, and there is no butyl rubber latex available commercially for emulsion compounding with alternative modifiers. Also, melt intercalation method using commercial organo-clays is the most practical method employed in the rubber and tire industry. No carbon black was used to discern the exclusive role of OMMTs in these compounds. Further, mechanical and dynamic-mechanical-thermal properties of the nano-composites were studied to

TABLE I
Base Recipe for Tire Curing Bladder Compound Without Carbon Black

Ingredients	phr	Function
Butyl rubber	95.0	Base elastomer
Polychloroprene rubber	5.0	Halogen activator
Zinc oxide	5.0	Catalyst
Stearic acid	1.5	Dispersing agent
Castor oil	5.0	Plasticizer and acid medium
Phenolic resin	6.0	Curing agent

phr, weight parts per 100 weight parts of rubber.

confirm the right selection of the OMMT for a butyl-based rubber nano-composite which has the potential application in tire curing bladders.

EXPERIMENTAL

Materials and methods

Butyl rubber (Butyl 301, Bayer), Polychloroprene (Baypren 210, Bayer), zinc oxide (Zno, Pars Techno), Stearic acid (Palmac1600, Acidchem), phenolic resin (Methyl phenol, SP1045, Schenectady) and castor oil (Pars Oil) were mixed according to the recipe given in Table I. Carbon black has been eliminated from the formulation for better studying of clay effects on compound's properties.

OMMT clays Cloisite10A, Cloisite15A, Cloisite20A, Cloisite25A, and Cloisite93A were supplied by Southern Clay Products Inc. The specifications of used OMMT modifiers in this work are shown in Table II.

Table III reports various commercial nano-clays and compositions used for this study and their designations. Melt intercalation method was employed for mixing compounds. Butyl rubber and Polychloroprene rubber were first melt blended at a temperature of 140°C in an internal mixer type Brabender N50EHT at 60 rpm for about five minutes. Then organo-clay, stearic acid and castor oil were added to the mixture and further mixed for 16 min. Processing temperature 140°C was chosen to avoid any significant thermal degradation of the organic modifier, specially seen at higher temperatures.[3] Incorporation of the curing agents took place on a laboratory two-roll mixing mill Brabender835800 with a friction ratio 2.8 and speed of 15 rpm.

Curing characteristics were obtained at 190°C by Rheometer. Rubber samples were cured at 190°C in an electrically heated hydraulic press at their optimum cure obtained from Rheometer. The basal spacing of the clay were studied by means of wide angle XRD in a scan range of $2\theta = 1$ to 10 degrees by a Philips X-Pert Pro diffractometer ($\lambda = 1.5418$ Å). Scanning Electron Microscopy (SEM) were performed using XL30 apparatus from Philips with excitation voltage of 20 kV. SEM Samples were cryogenically fractured, and fractured surfaces were spotter coated with gold before microscopy. AFM on the surface of samples was performed using DME SPM-Prober Station 150 with a pyramidal silicone tip resonating at 260 kHz in a soft tapping mode. Mechanical properties in the tension mode were measured in a uni-axial tensile machine, Instron series 5565, according to the standard ASTM D412. Dynamic Mechanical Thermal Analysis (DMTA) were performed on the samples in a temperature sweep from −150 °C to +150 °C at frequency of 1 Hz, strain of 0.2% in a single cantilever bending mode (DMA-Triton, Tritec 2000, Triton technology).

RESULTS AND DISCUSSIONS

Vulcanization characteristics of nano-composites

Vulcanization characteristics of the nano-composites prepared with different organically-modified clays are shown in Table IV and compared with the base compound (rubber compound without OMMT). Minimum and maximum torques of all samples

TABLE II
Modifier Specifications for Used Montmorillonites

Commercial name	Cloisite10A	Cloisite15A	Cloisite20A	Cloisite25A	Cloisite93A
Modifierstructure	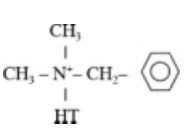	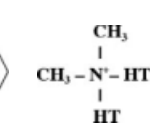	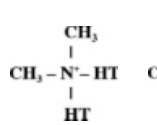	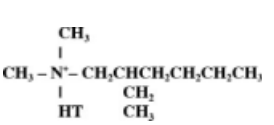	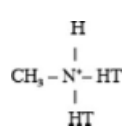
Modifierchemicalname	2MBHT	2M2HT	2M2HT	2MHTL8	M2HT
Anion	Chloride	Chloride	Chloride	methyl sulfate	HSO4
Modifier concentration (meq/100 g clay)	125	125	95	95	90

HT, Hydrogenated tallow (~65% C18; ~30% C16; ~5% C14); 2MBHT, dimethyl, benzyl, hydrogenated tallow, quaternary ammonium; 2M2HT, dimethyl, dehydrogenated tallow, quaternary ammonium; 2MHTL8, dimethyl, dehydrogenated tallow, 2-ethylhexyl quaternary ammonium; M2HT, methyl, dehydrogenated tallow ammonium.

TABLE III
Designation of Rubber Compounds, Organo-Clays, and Their Nano-Composites

Composition	Designation
Base recipe for tire curing bladder compound without Organo-clay	Ru
Cloisite10A	10A
Base recipe +4% Cloisite10A	R 10A
Cloisite15A	15A
Base recipe +4% Cloisite15A	R 15A
Cloisite20A	20A
Base recipe +4% Cloisite20A	R 20A
Cloisite25A	25A
Base +4% Cloisite25A	R 25A
Cloisite93A	93A
Base +4% Cloisite93A	R 93A

increase when organo-clays are added to the base compound. This shows the reinforcing effect of these fillers in the rubber compounds. Also, scorch and optimum cure times are longer when organo-clay is present in the compound. This is contrary to what has been seen for vulcanization of rubber-organo-clay nano-composites with sulfur cure systems where amine chemical groups activate the curing process.[9] While acid medium helps to activate Phenolic cross-linking systems, retardation in vulcanization can be attributed to deactivation of Ricinoleic Acid (caster oil) and Polychloroprene activators by basic amine groups present in the modified clay, so hindering the accelerating effect of these activators.[26]

Evaluation of degree of intercalation by XRD

The degree of dispersion of the silicates can be estimated through intercalation of rubber into layer spacing of the silicate platelets by XRD. Figure 1a–c compare the X-ray diffractographs of pure organo-clays, rubber-clay nano-composites before vulcanization, and these nano-composites after vulcanization, respectively. As a measure of rubber intercalation into the galleries of silicate layers and increase in d-spacing of these layers, shift in position of (001) peaks can be detected and related to the corresponding d-spacing according to Bragg's law.[1,2] The d-spacing of the organo-clays before and after dispersing into the nano-composites and their corresponding differences are summarized in Table V. Considering this table, intercalation of rubber into the clay interlayer spacing was confirmed by shift in (001) peak in all of the nano-composites. Although starting with different initial d-spacing, all organo-clay's structures reach similar final d-spacing in nano-composites, and Cloisite10A shows the highest value of d-spacing among others. More important than the final d-spacing is the change in this parameter, as indicated in Table V as Δd_{001}. The latter parameter is a measure of the interaction of rubber into the spacing of the silicate layers, disregarding the initial degree of opening introduced by the modifier. Among all the organo-clays employed in this study, Cloisite10A demonstrate the highest gallery opening as well as Δd_{001}, thus the best dispersion in the rubber matrix. However, there is no indication of considerable exfoliated structure of organo-clays in these nano-composites from XRD.

Comparing Figure 1(b,c), one can notice presence of the peaks at higher angles for all vulcanized nano-composites, especially for R93A and R25A, compared to those of corresponding unvulcanized ones. This has been correlated to deintercalation of rubber out of some silicate interlayer spacing due to either degradation of modifiers and collapse of layers or larger entropy of rubber chains during vulcanization process.[34,35] However, there is not much difference in intensity and position of such peaks for R10A, indicating stability and compatibility of the corresponding organo-clay in this nano-composite.[3] Also, it is noticeable the loss of magnitude and slight shift of the (001) peak to lower angles for R10A, compared to other nano-composites. This also suggests loss of order in already intercalated structure of 10A organo-clay during vulcanization. Such post disordered-intercalated structure can be attributed to diffusion of phenolic resin into the gallery spacing of the silicates and vulcanization of rubber in this region. Exact values of d-spacing and their changes during vulcanization process are reported in Table V.

DMTA of vulcanized nano-composites

Dynamic-mechanical properties of the base vulcanizate and its nano-composites were studied in a temperature sweep over a wide range. The loss factor (tan δ) as a function of temperature for all of the nano-composites and the base compound is plotted

TABLE IV
Cure Characteristics of the Base Compound and Nano-Composites

	Ru	R 10A	R 15A	R 20A	R 25A	R 93A
Minimum torque (N.m)	2.90	4.14	3.37	3.95	4.15	4.01
Maximum torque (N.m)	4.17	6.84	5.96	6.09	6.37	8.10
Scorch time, T2 (Min)	0.19	1.40	2.59	2.00	2.20	2.00
Optimum cure,T90 (Min)	14.60	19.11	15.53	20.90	16.90	27.50

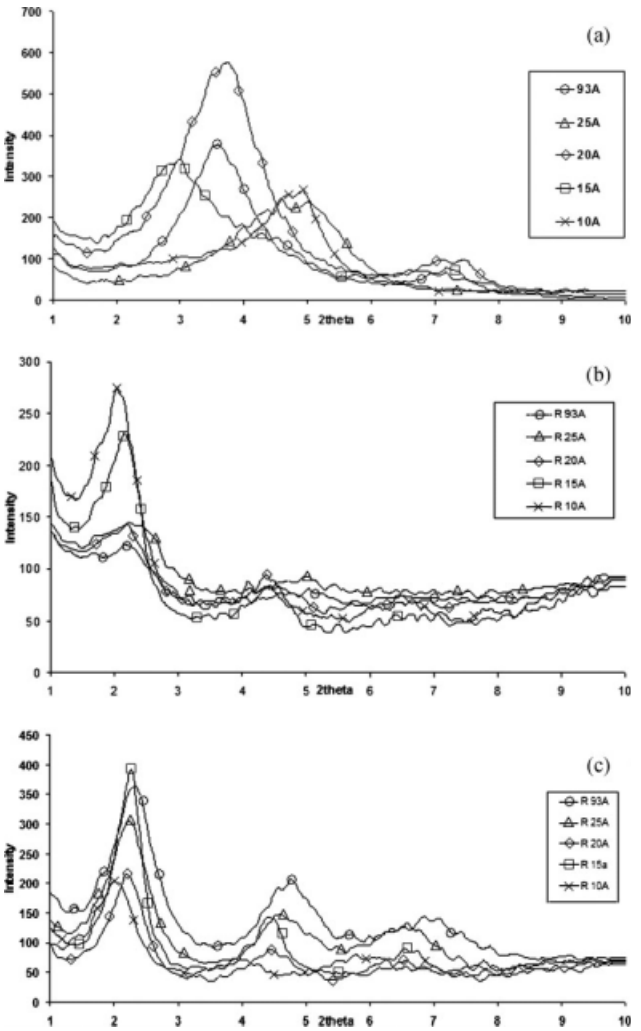

Figure 1 X-ray diffractographs of (a) pure organo-clays, (b) nano-composites containing organo-clays before vulcanization, and (c) nano-composites containing organo-clays after vulcanization.

in Figure 2. The variation of tan δ peak, glass transition temperature (T_g) and Storage modulus (at 25°C) for the nano-composites with respect to those for the base compound are shown in Table VI. The peak of loss factor, corresponding to the glass transition temperature (T_g) of the elastomer is reduced by adding the organo-clays, and this effect is more noticeable in the case of the noano-composite containing Cloisite10A. This can be attributed to immobilization of the rubber chains in the form of shell and/or trapped rubber, causing reduction of the free polymer volume fraction in the presence of filler.[36] That is, at low temperatures the polymer by itself is responsible for a high proportion of energy dissipation, while the small solid filler particles and the immobilized rubber around them hardly absorb any energy.[36] Furthermore, a shift in glass transition temperature (peak tanδ) to higher temperatures upon addition of the filler suggests that there exists adhesion at the filler/polymer interface, in particular, in the case of the composite of Cloisite10A. This elevation in glass transition temperature is again due to polymer-filler interaction which restricts the mobility of the elastomer segments. In general, both shifts in peak tanδ are indications of rubber reinforcement by the filler, especially by the best dispersed Cloisite10A. In this study, the results obtained are in agreement with the general tendency reported in the literature.[36]

Figure 3 shows the storage modulus of nano-composites as a function of temperature. As it can be observed, the organo-clay gives rise to a noticeable increase in modulus of the base compound over the whole range of temperature. The magnified graph clearly shows this increase in the storage modulus in the rubbery region as well. As indicated in Table VI, Cloisite10A shows the highest value of storage modulus at room temperature) (25°C) with about 57% increase compared to that for the unfilled compound (Ru). This behavior is due to hydrodynamic as well as strain amplification arising from the incorporation of solid inclusions into the elastomeric matrices.[36] The hydrodynamic effect mainly depends on two factors, the volume fraction and the high aspect ratio of silicate platelets. On the other hand, it is assumed that the greater the dispersion of filler, the larger is its contact with rubber chains, thus the reinforcing effect. Also, the portion of rubber chains trapped in the filler as a result of mixing (rubber portion immobilized or occluded) act as a part of the filler rather than of the polymer and hence, the effective volume of the filler increases.[37,38]

TABLE V
d-Spacing of the Organo-Clays Before and After Dispersion in the Nano-Composites and Vulcanization

		10A	15A	20A	25A	93A
Pure organo-clay	d_{001} (nm)	1.76	2.94	2.35	1.92	2.45
Nano-composites containing organo-clays before vulcanization	d_{001} (nm)	4.28	4.06	3.96	3.91	4.01
	Δd_{001} (nm) After mixing–before mixing (rubber intercalation)	2.515	1.116	1.612	1.992	1.562
Nano-composites containing organo-clays after vulcanization	d_{001} (nm)	4.34	3.84	3.97	3.89	3.73
	Δd_{001} (nm) After vulcanization–Before vulcanization	0.062	−0.216	0.002	−0.017	−0.282

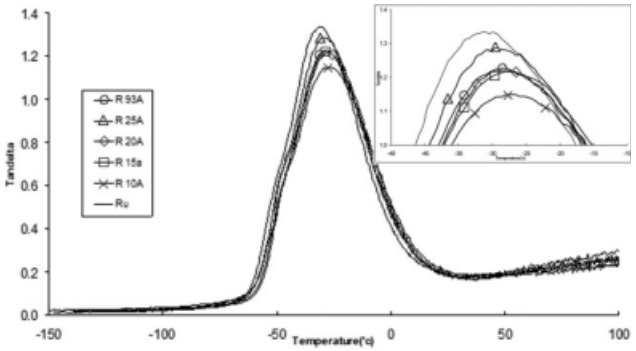

Figure 2 Loss factor for the nano-composites and the base compound in a temperature sweep.

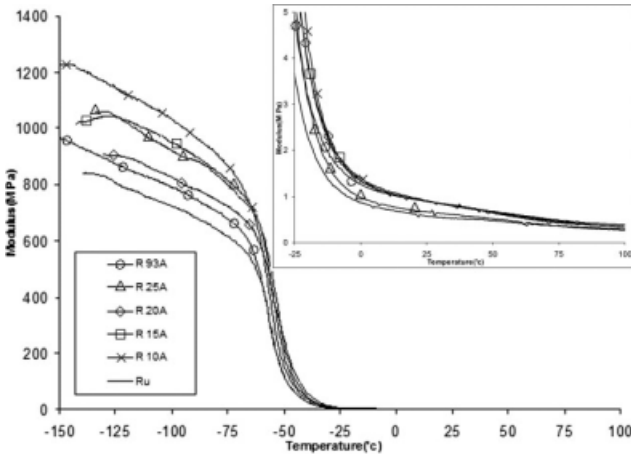

Figure 3 Storage modulus of nano-composites and the base compound.

In the case of studied organo-clays, Cloisite10A shows the highest interaction with the compound and the largest degree of reinforcement. This is in agreement with the XRD results showing larger extent of intercalated structure and dispersion of Cloisite10A in the rubber matrix studied. The better compatibility of this organo-clay with the bladder base compound can be attributed to the miscibility of Cloisite10A modifier and the rubber matrix consisting of butyl rubber and chloroprene. Because of presence of benzyl group in the 2MBHT modifier, this organo-clay is partially more polar than the other organo-clays with hydrocarbon groups. On the other hand, presence of chloroprene in the compound as the activator of curing system provides more polarity to the rubber matrix than pure butyl rubber. Also, phenolic resin as the curing agent has more compatibility with the 2MBHT modifier, which in turn may enhance assimilation of Cloisite10A in this rubber compound.

Morphological studies of selected nano-composite

According to XRD and DMTA, the nano-composite R10A was selected as the compound of choice for possible application in curing bladder. Although there was no elimination of (001) peak in XRD diffractographs of this nano-composite and less chance of fully exfoliated structure, large shift along with loss of magnitude in broadened peak of the vulcanized compound may hint on partially exfoliated structure of this nano-composite. To study the morphology of this nano-composite, first SEM micrographs were obtained, as shown in Figure 4(a,b) in two different scales. Submicron white dots are clay aggregates properly distributed in the gray rubber matrix, as observed in Figure 4(a). The light large bumps on the surface are fracture ridges in this figure. Aggregates of clay are more magnified in Figure 4(b). In this figure, white spots are clay agglomerates, and the size of particle with a cross on it was measured to be 64-nm thick and 418 nm long, as recorded at the bottom of this figure. Only clay agglomerates appear in the SEM micrographs, and there is no evidence of intercalated or possible partially exfoliated clay structure in or around the agglomerates. For further investigation, AFM micrographs were obtained, as shown in Figure 5(a,b). These figures are in 1.0 micron scale, showing phase [Fig. 5(a)] and height [Fig. 5(b)] images. At the lower section of the phase image, white area in the form of lines and dots represent hard phase of clay dispersed in the matrix of rubber and soft oil-swollen rubber.[19] The same area in the height image confirms the presence of clay bundles. These figures show that clay bundles with thickness of about 10 nm are separated by intercalating rubber. The circle in the height image highlights some isolated thin bundles with their corresponding white lines in the phase image. The clay in this area may be some partially exfoliated structure around the clay agglomerate located at the corner of the micrograph. The intercalated or partially exfoliated structure of filler

TABLE VI
Variations in Magnitude and Position of Peak Loss Factor (Tan δ) and Variations in Magnitude of Storage Modulus (at 25°C) for the Nano-Composites

	Ru	R 10A	R 15A	R 20A	R 25A	R 93A
Magnitude of peak tan δ	1.334	1.149	1.218	1.220	1.288	1.227
Reduction in peak tan δ	0	−0.185	−0.116	−0.114	−0.046	−0.107
Glass transition temperature (°c)	−31.2	−27.0	−28.0	−28.3	−29.5	−28.6
Shift in glass transition temperature	0	4.2	3.2	2.9	1.7	2.6

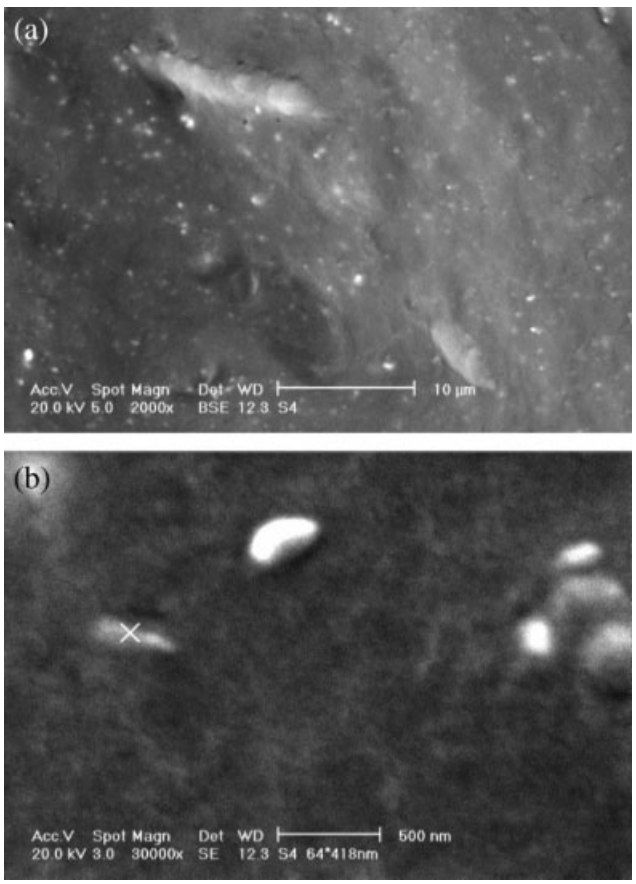

Figure 4 SEM micrographs of fractured surface of R10A nano-composite. (a) scale = 10 micrometer (b) scale = 500 nanometer.

is responsible for shift of (001) peak in the XRD diffractographs along with loss of magnitude and broadening after mixing in rubber and vulcanization process.

Mechanical properties of nano-composites

Typical tension curves obtained from tensile test for all nano-composites and the base vulcanizate are

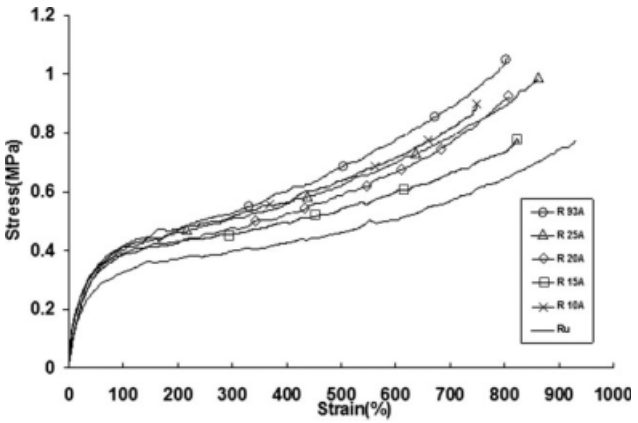

Figure 6 Stress–strain curves for nano-composites and the base compound.

shown in Figure 6. Elastic modulus in the whole strain range is remarkably increased in nano-composites compared to that of the base compound. Figure 7(a–d) compare the stress at certain strains for all samples. Tensile strength and elongation at break were not recorded since the specimens did not break until the maximum range of the tensile machine reached (900% strain).

Results show that Cloisite10A and Cloisite93A impart rather higher reinforcement and moduli to the rubber nano-composites than other modified clays.

CONCLUSIONS

A series of vulcanized butyl-based nano-composites containing different OMMT nano-clays obtained by melt blending were studied. The optimum cure time was increased in the presence of organo-clays in all of studied samples due to basic nature of the clay modifiers in the acid-activated phenolic cure system. XRD results showed intercalation of rubber chains into the clay interlayer spacing for all of the nano-composites, and the maximum opening in gallery

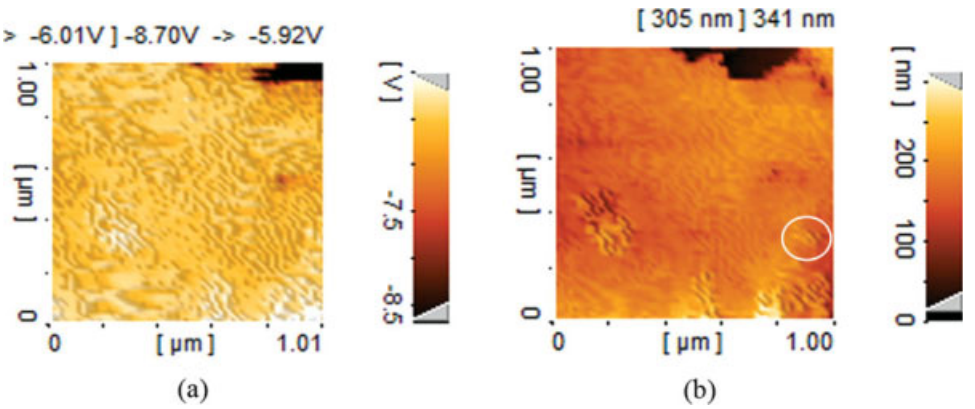

Figure 5 AFM micrographs from the surface of R10A nano-composite (a) phase image (b) height image. [Color figure can be viewed in the online issue, which is available at www.interscience.wiley.com.]

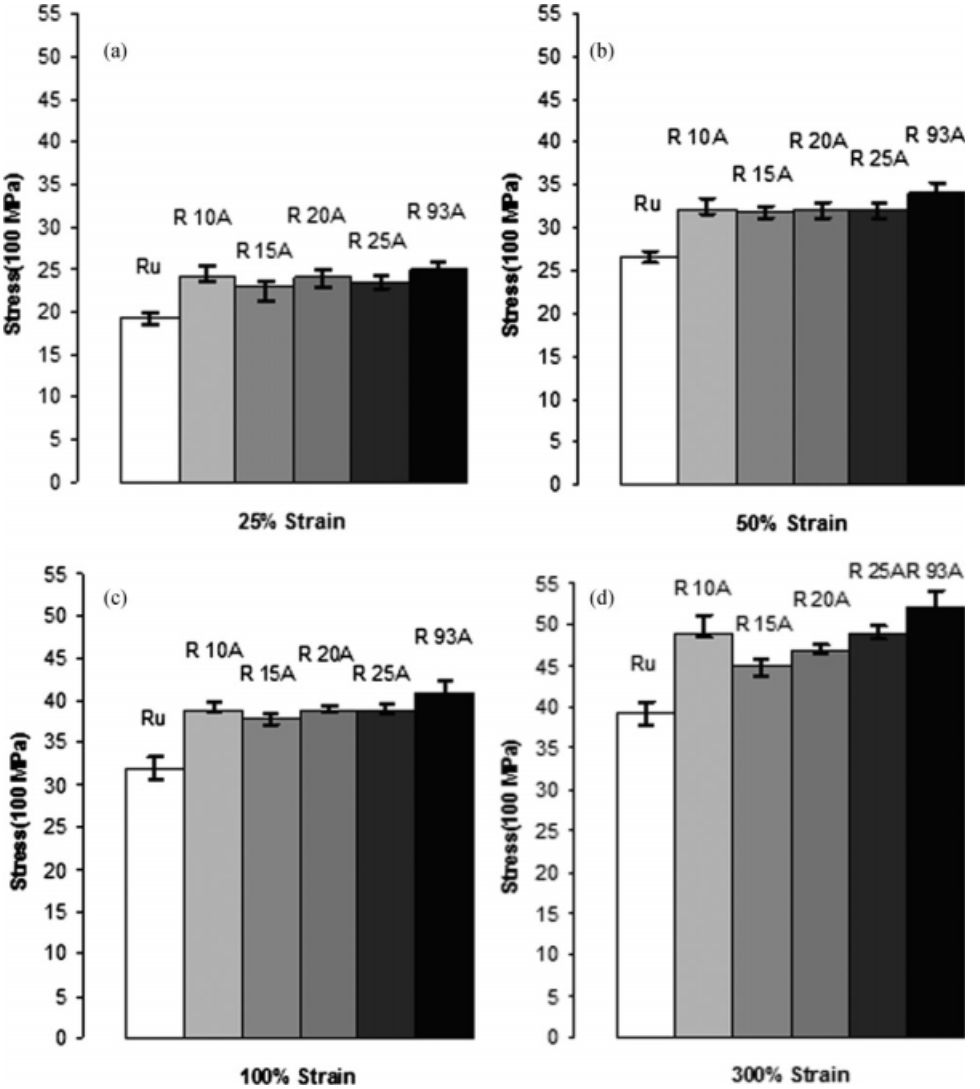

Figure 7 Stress at certain strains for nano-composites and the base compound: (a) 25%, (b) 50%, (c) 100%, and (d) 300% strain.

height was observed for the composite of Cloisite10A in the studied rubber compound. Also, vulcanization process did not reduce spacing of the silicate layers in the latter case. Dispersion and distribution of this nano-composite obtained by SEM and AFM confirmed intercalated and possible partially exfoliated structure of this OMMT in the butyl-based rubber compound. Using dynamic-mechanical loss factor as a measure of rubber-clay interaction, the magnitude of peak loss factor for all nano-composites is reduced and their glass transition temperature shifted to higher temperatures. Among all nano-composites, the one prepared by Cloisite10A showed the highest interaction and reinforcement effect with this rubber compound due to chemical nature of its modifier. Finally, tensile moduli of all nano-composites were higher than those of the base rubber with no organo-clay. As a result, Cloisite10A organo-clay was chosen as the most efficient reinforcing clay for further study of effect of this organo-clay on properties of butyl-based bladder rubber compounds.

References

1. Alexandre, M.; Dubois, P. Mater Sci Eng 2000, 28, 1.
2. Ray, S. S.; Okamoto, M. Prog Polym Sci 2003, 28, 1539.
3. Utracki, L. A. Clay-Containing Polymeric Nanocomposites; Smithers Rapra Technology Limited: United Kingdom, 2004.
4. Razzaghi-Kashani, M.; Hasankhani, H.; Kokabi, M. Iranian Polym J 2007, 16, 671.
5. Lai, M. C.; Chang, K. C.; Yeh, J. M.; Liou, Sh. J.; Hsieh, M. F.; Chang, H. S. Euro Polym J 2007, 43, 4219.
6. Changa, K. C.; Jang, G. W.; Peng Ch, W.; Lin, C. Y.; Shieh, J. C.; Yeh, J. M.; Yang, J. C.; Li, W. T. Electrochim Acta 2007, 52, 5191.
7. Liu, Y. D.; Choi, H. J. J Mater Sci 2009, 44, 2999.
8. Song, D. H.; Lee, H. M.; Choi, H. J. J Nanosci Nanotech 2009, 9, 1501.

9. Cataldo, F. Macromol Symp 2007, 247, 67.
10. Meneghetti, P.; Qutubuddin, S. Thermochem Acta 2006, 442, 74.
11. Jeona, H. S.; Rameshwarama, J. K.; Kimb, G.; Weinkauf, D. H. Polymer 2003, 44, 5749.
12. Vaia, R. A.; Giannelis, E. P. Macromolecules 1997, 30, 8000.
13. Jia, Q. X.; Wu, Y. P.; Wang, Y. Q.; Lu, M.; Yang, J.; Zhang, L. Q. J Appl Polym Sci 2007, 103, 1826.
14. Vaia, R. A.; Ishii, H.; Giannelis, E. P. Chem Mater 1993, 5, 1694.
15. Gilman, J. W.; Jackson, C. L.; Morgan, A. B.; Harris, R. Chem Mater 2000, 12, 1866.
16. Morgan, A. B.; Gilman, J. W. J Appl Polym Sci 2003, 87, 1329.
17. Schmidt, D. F. Ph.D. Thesis, Cornell University, 2003.
18. Vaia, R. A.; Liu, W.; Koerner, H. J Polym Sci Part B: Polym Phys 2003, 41, 3214.
19. Sadhu, S.; Bhowmick, A. K. J Mater Sci 2005, 40, 1633.
20. Karger, L. J Polym Eng Sci 2004, 44, 1083.
21. Xi, Y.; Ding, Z.; He, H.; Frost, R. L. J Colloid Interface Sci 2004, 277, 116.
22. Lertwimolnun, W.; Vergnes, B. Polymer 2005, 46, 3462.
23. Fornesa, T. D.; Yoona, P. J.; Hunterb, D. L.; Keskkulaa, H.; Paul., D. R. Polymer 2002, 43, 5915.
24. Tiwari, R. R.; Natarajan, U. J Appl Polym Sci 2007, 105, 2433.
25. Ma, J.; Xiang, P.; Mai, Y.-W.; Zhang, L.-Q. Macromol Rapid Commun 2004, 25, 1692.
26. Kim, W.; Kang, B.-S.; Cho, S.-G.; Hac, S.; Bae, J.-W. Composite Interfaces 2007, 14, 409.
27. Kuo, W.-F.; Wu, J.-Y.; Lee, M.-S.; Lee, S.-Y. U.S. Pat. 6,710,111 B2 (2004).
28. Yang, X.; Cohen, M. P.; Senyek, M. L.; Parker, D. K.; Cronin, S. W.; Lukich, L. T.; Francik, W. P.; Gurer, C. U.S. Pat. 7,342,065 B2 (2008).
29. Ma, J.; Yu, Z.-Z.; Kuan, H.-C.; Dasari, A.; Mai, Y.-W. Macromol Rapid Commun 2005, 26, 830.
30. Sreekanth, B. P.; Shriharsha, B.; Raghavendra, D.; Ananthapadmanabha, G. S.; Shashidhara, G. M. Polym Int 2000, 49, 1684.
31. Majumdar, S.; Reddy, G. R. Exel Rubber Limited: Hyderabad, 2000.
32. Lietz, S.; Yang, J. L.; Bosch, E.; Sandler, J. K. W.; Zhang, Z.; Altstadt, V. Mater Eng 2007, 292, 23.
33. Warholid, T. C.; Pelle, R. G. Tire Sci Technol 1988, 16, 128.
34. Gatos, K. G.; Sza'zdi, L.; Puka'nszky, B.; Karger-Kocsis, J. Macromol Rapid Commun 2005, 26, 915.
35. Liang, Y. R.; Ma, J.; Lailu, Y.; Wu, Y. P.; Zhang, L. Q.; Mai, Y. W. Polym Phys 2005, 43, 2653.
36. Lo'pez-Manchado, M. A.; Herrero, B.; Arroyo, M. Polym Int 2004, 53, 1766.
37. Boonstra, M. M. Polymer 1979, 20, 691.
38. Maiti, M.; Bhowmick, A. K. Polym Eng Sci 2007, 47, 1777.